Bioorganic & Medicinal Chemistry Letters 21 (2011) 3050–3056

Contents lists available at ScienceDirect

Bioorganic & Medicinal Chemistry Letters

journal homepage: www.elsevier.com/locate/bmcl

The discovery of novel benzofuran-2-carboxylic acids as potent Pim-1 inhibitors

Yibin Xiang [a,*], Bradford Hirth [a], Gary Asmussen [b], Hans-Peter Biemann [b], Kimberly A. Bishop [e], Andrew Good [a], Maria Fitzgerald [c], Tatiana Gladysheva [b], Annuradha Jain [e], Katherine Jancsics [a], Jinyu Liu [b], Markus Metz [a], Andrew Papoulis [a], Renato Skerlj [a], J. David Stepp [b], Ronnie R. Wei [d]

[a] Department of Medicinal Chemistry, Drug and Biomaterial R&D, Genzyme Corp., 153 Second Avenue, Waltham, MA 02451, USA
[b] Department of In Vitro Biology, Drug and Biomaterial R&D, Genzyme Corp., 153 Second Avenue, Waltham, MA 02451, USA
[c] Department of DMPK, Drug and Biomaterial R&D, Genzyme Corp., 153 Second Avenue, Waltham, MA 02451, USA
[d] Department of Therapeutic Protein Research, Genzyme Corp., 1 Mountain Road, Framingham, MA 01701, USA
[e] Department of Therapeutic Protein Discovery, Genzyme Corp., 49 New York Ave, Framingham, MA 01701, USA

ARTICLE INFO

Article history:
Received 8 February 2011
Revised 7 March 2011
Accepted 9 March 2011
Available online 16 March 2011

Keywords:
Enzyme,
Kinase
Inhibitor
Benzofuran
X-ray structure
Structure based design
Salt-bridge
Hydrogen bond interaction
Synthesis
Carboxylic acid
Amine
Basicity
SPR
Medicinal chemistry
Fragment screening

ABSTRACT

Novel benzofuran-2-carboxylic acids, exemplified by **29**, **38** and **39**, have been discovered as potent Pim-1 inhibitors using fragment based screening followed by X-ray structure guided medicinal chemistry optimization. The compounds demonstrate potent inhibition against Pim-1 and Pim-2 in enzyme assays. Compound **29** has been tested in the Ambit 442 kinase panel and demonstrates good selectivity for the Pim kinase family. X-ray structures of the inhibitor/Pim-1 binding complex reveal important salt-bridge and hydrogen bond interactions mediated by the compound's carboxylic acid and amino groups.

The Pim-1 serine/threonine kinases and its two other family members, Pim-2 and Pim-3 are associated with several oncogenic processes.[1] The *pim-1* proto-oncogene was initially identified as a frequent site of integration for slowly transforming Maloney murine leukemia virus in murine T cell lymphomas.[2] Recently, Pim-1 associated regulation of the c-myc, antiapoptotic protein BAD and p27kip1 have also been described.[3] Pim-1 overexpression is observed in a range of human lymphomas and acute leukemia,[4] whereas Pim-2 overexpression is associated with chronic lymphocytic leukemia and non-Hodgkin lymphoma.[5] Leukemias driven by mutationally-activated FLT3 comprise a proposed indication because Pim kinases are transcriptionally activated by FLT3.[6] Structural evidence corroborates this mode of activation as Pim kinases appear to be constitutively activated enzymes in contrast to the more common type kinases which are activated by phosphorylation.[7] Another structural feature of interest is the presence of an unusual proline in the hinge region of ATP binding site, that not only expands the ATP pocket but also alters the kinase hinge hydrogen bonding motif. Such unique features implicate the potential of finding small molecules which may selectively inhibit the enzyme by binding to the ATP binding pocket of the Pim kinase family.

The pleiotropic roles of Pim family kinases in proliferation and survival pathways have attracted interest of many investigators to the discovery of inhibitors as potential therapeutics. In the last a few years, a number of potent Pim-1 inhibitors have been reported in the literature.[8] Figure 1 illustrates examples of these compounds which include substituted fused triheterocycles (**1** and **2**), a disubstituted pyrazine (**3**), a disubstituted pyridine (**6**) and disubstituted fused diheterocycles (**4**, **5**, **7** and **8**).

As part of a Genzyme drug discovery program aimed at identifying protein kinase inhibitors as potential therapeutics for cancer

* Corresponding author.
E-mail address: yibin.xiang@genzyme.com (Y. Xiang).

0960-894X/$ - see front matter © 2011 Elsevier Ltd. All rights reserved.
doi:10.1016/j.bmcl.2011.03.030

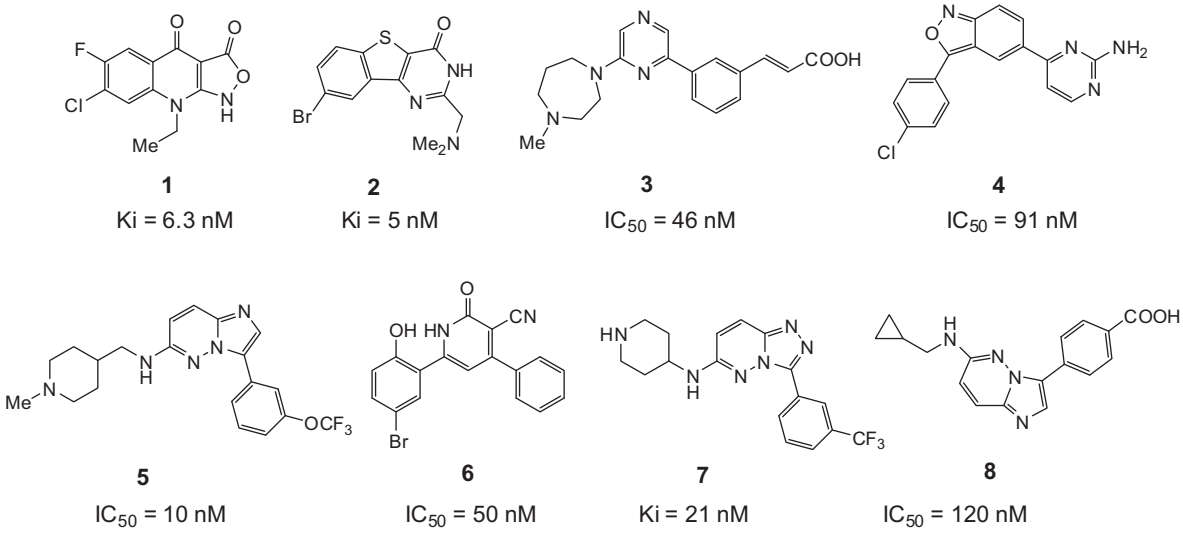

Figure 1. Inhibitors of Pim-1 kinase and the reported IC_{50} or K_i values.[8]

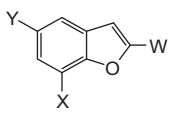

9	Y = H, X = H,	W = COOH;	IC_{50} = 119 uM	LE: 0.45
10	Y = Br, X = H,	W = COOH;	IC_{50} = 8.5 uM	LE: 0.54
11	Y = Br, X = OMe,	W = COOH;	IC_{50} = 5.8 uM	LE: 0.48
52	Y = Br, X = OMe,	W = CN;	No inhibition at 25 uM	

Figure 2. Pim-1 inhibitors identified by SPR screening.[9] The IC_{50}s were determined in a Pim-1 biochemical assay.[10]

treatment, we selected Pim-1 as a target of interest. Our strategy involved using fragment based screening to find early hit molecules, which would then be optimized by X-ray structure guided medicinal chemistry optimization to improve their potency and selectivity. In the pursuit of finding Pim-1 inhibitors, approximately 1800 fragment molecules (molecular weights in the range of 150–300 D) were screened for binding activity to Pim-1 using Surface Plasmon Resonance (SPR) at 75 μM followed by determination of steady-state binding affinities of the hits to confirm binding.[9] The active compounds were then evaluated in a Pim-1 biochemical assay by measuring IC_{50} values.[10] Among many active compounds identified through this process, a few derivatives of benzofuran-2-carboxylic acid were of special interest. As illustrated in Figure 2, compound **9** did not exhibit potent inhibition of Pim-1, however, derivatives of **9** with a bromo substituent at the 5-position (**10** and **11**) demonstrated a significant 12–20-fold increase in activity. The ligand efficiency (LE) of compounds **10** and **11** is 0.54 and 0.48, respectively (Fig. 2), which are attractively high.[14] To the best of our knowledge, no benzofuran-2-carboxylic acid derivatives have been reported in the literature as potent Pim-1 inhibitors. Compounds **10** and **11** were soaked into Pim-1 crystals and the structures of the binding complexes were determined (Fig. 3).[11] In both structures, the bromo group of **10** or **11** is sitting in a hydrophobic pocket created by hinge *P125* and surrounded by *A65*, *R122*, *L44* and *L174*. This hydrophobic interaction likely provides a significant contribution to Pim-1 binding and inhibition because analog **9**, which lacks the bromo substituent

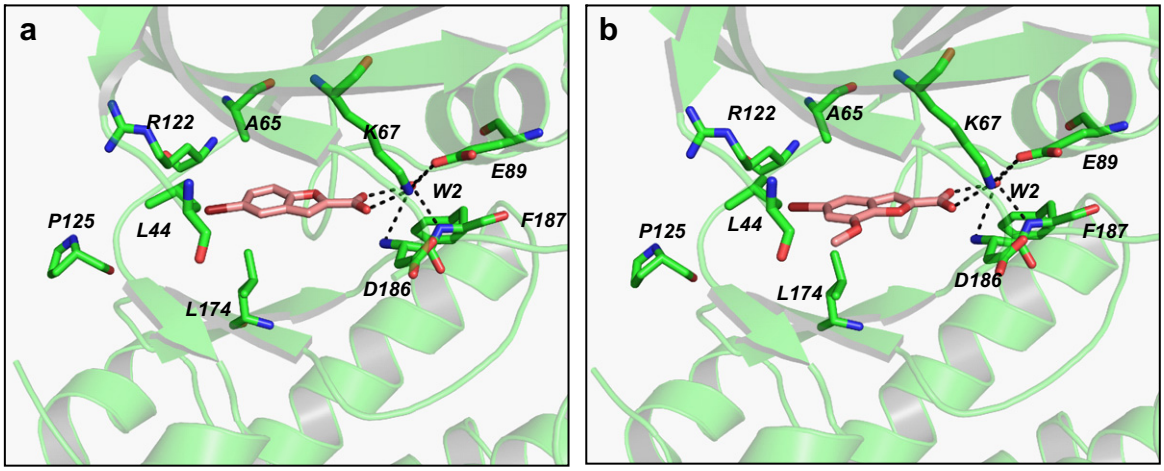

Figure 3. (a) X-ray structure of compound **10** binding to the ATP site of Pim-1. (b) X-ray structure of compound **11** binding to the ATP site of Pim-1. In both structures, the bromo groups of **10** and **11** are located in the hydrophobic pocket surrounded by *A65*, *R122*, *L44* and *L174*, and the 2-carboxylic acid group forms the salt-bridge interactions with *K67* and hydrogen bond interactions through the water molecule with *E89* and *D186*. The orientation of the benzofuran core of compound **10** and **11** are almost 180° opposite to each other.

Table 1
Pim-1 and Pim-2 enzymatic inhibition by 5-substituted benzofuran-2-carboxylic acids

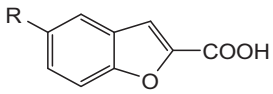

	R	IC_{50}[a] (μM)					IC_{50}[a] (μM)		
		Pim-1	Pim-2	LE[b]			Pim-1	Pim-2	LE[b]
12	F_3C–	5.3	13.5	0.45	**19**	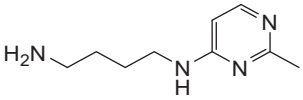	1.9	1.2	0.33
13	F_3CO–	6.1	NT	0.42	**20**	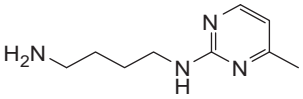	0.46	0.59	0.37
14		7.8	7.1	0.39	**21**	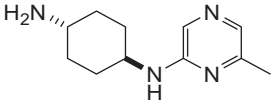	0.12	0.054	0.37
15		7.4	11.9	0.39	**22**	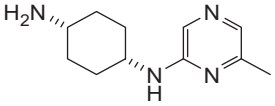	0.20	0.11	0.36
16	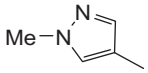	5.4	2.9	0.40	**23**	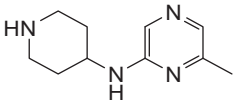	0.21	0.15	0.37
17	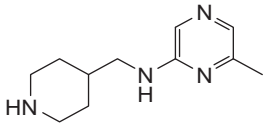	0.38	0.16	0.34	**24**	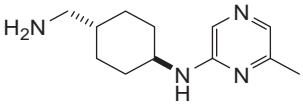	0.053	0.021	0.37
18	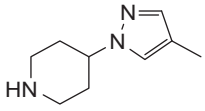	6.0	5.8	0.31	**25**	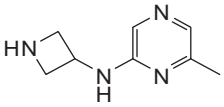	0.45	0.10	0.38

[a] Concentration of the testing compounds to inhibit 50% activity of the target enzymes.[10] The values of IC_{50} are means of at least two independent experiments.
[b] Ligand efficiency.[14]

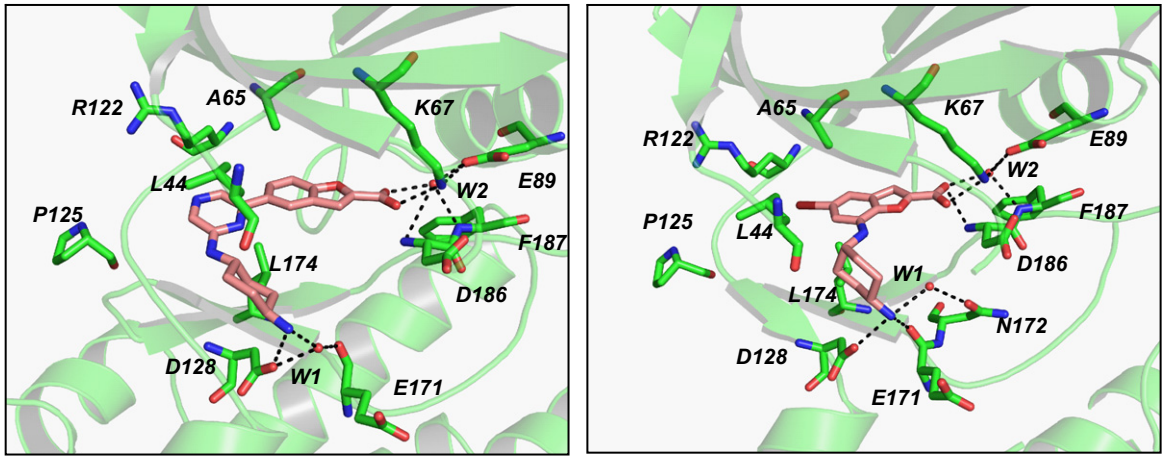

Figure 4. (a) X-ray structure of compound **21** binding to the ATP site of Pim-1. The pyrazine sits in the position which was partially occupied by the bromo group of compound **10** (see Fig. 3a). The terminal amino group of the *trans*-diaminocyclohexanyl moiety forms a salt-bridge interaction with *D128* and hydrogen bond interactions with *E171* mediated by a water molecule; (b) X-ray structure of compound **38** binding to the ATP site of Pim-1. The terminal amino group of the *cis*-diaminocyclohexanyl moiety forms salt-bridge interactions with *D128* and *E17 and a* hydrogen bond interaction with *N172* through a water molecule, while the 5-bromo substituent sits in the hydrophobic pocket near the hinge region.

at the 5-position, demonstrates only limited inhibitory activity (Figure 2). The 2-carboxylic acid group forms a salt-bridge interaction with *K67* and hydrogen bond interactions (mediated by a water molecule) to the amino acids *E89* and *D186*. All the three amino acids are highly conserved among many protein kinases. The importance of this interaction is demonstrated by compound

52. It contains a cyano group at the 2-position rather than carboxylic acid group, which is thus rendered inactive at a concentration of 25 μM (Fig. 2). It is interesting to note from the X-ray crystal structures that the orientation of the benzofuran core of compounds **10** and **11** is inversed almost 180°, while the bromo group remains sitting in almost the same position within the hydrophobic pocket. The structural features of the binding complexes of **10** and **11** and the SAR of **9**, **10**, **11** and **52** lead to several key considerations: (a) hydrophobic interactions between a substituent at the 5-position of the benzofuran and the hydrophobic pocket of the Pim-1 hinge region may contribute significantly to binding; (b) the salt-bridge interaction mediated by the 2-carboxylic acid group to *K67* and hydrogen bond interactions with *E89* and *D186* could define another important binding site; (c) there is little tolerability for additional substituents near the gate keeper site and (d) a potential space exits for structural expansion at the ribose binding region.

In view of this knowledge, two approaches were proposed and examined in an attempt to improve the potency of these early hits: replacing either the 5-bromo substituent of compound **10** or the 7-methoxy group of compound **11** with an extended linker fragment containing a basic moiety to capture additional interactions with acidic amino acid residues in the ribose binding region, while maintaining the benzofuran core and 2-carboxylic acid group unchanged. The potential attribution of hydrogen bond interactions with the acidic amino acid residues in the ribose binding region was reported by Qian and his coworkers in their publication in 2009.[8c]

Table 1 illustrates analogs derived from compound **10** and their activities against Pim-1 and Pim-2. As expected, the 5-position of the benzofuran core can tolerate other hydrophobic groups, such as trifluoromethyl (**12**) or trifluoromethoxy (**13**) moieties evidenced by that these compounds are equipotent to **10**. Replacing the 5-bromo group with a nitrogen containing heterocycle, such

Table 2
Pim-1 and Pim-2 enzymatic inhibition by 5-bromo-7-substituted benzofuran-2-carboxylic acids

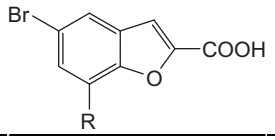

	R	IC_{50}[a] (μM)				R	IC_{50}[a] (μM)		
		Pim-1	Pim-2	LE[b]			Pim-1	Pim-2	LE[b]
26	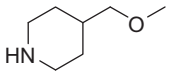	0.060	0.25	0.47	**35**	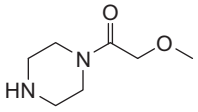	0.22	1.3	0.40
27	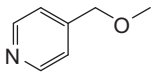	4.9	12.5	0.35	36	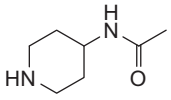	0.98	7.0	0.38
28	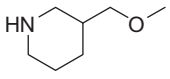	0.071	0.33	0.47	37	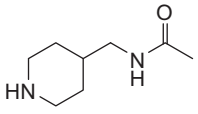	2.7	1.3	0.33
29	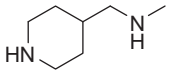	0.020	0.19	0.50	38	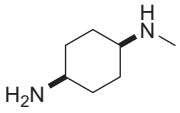	0.001	0.004	0.59
30	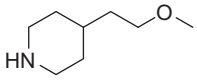	0.051	0.35	0.46	39	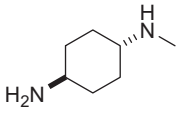	0.019	0.066	0.50
31	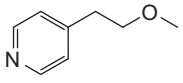	4.5	21.1	0.33	**40**	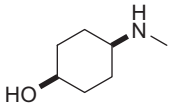	2.3	6.8	0.37
32	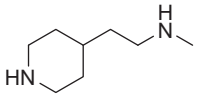	0.040	0.54	0.46	41	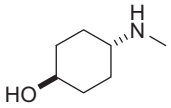	2.4	6.1	0.37
33	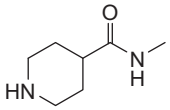	0.15	0.26	0.43					
34	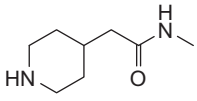	0.055	0.34	0.43					

[a] Concentration of the testing compounds to inhibit 50% activity of the target enzymes.[10] The values of IC_{50} are means of at least two independent experiments.
[b] Ligand efficiency.[14]

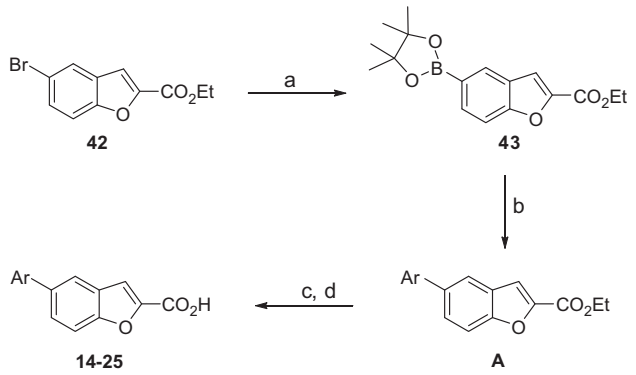

Scheme 1. Reagents and conditions: (a) bis(pinacolato)diboron, $Pd(OAc)_2$, tricyclohexylphosphine, CsF, ACN, reflux (75%); (b) aryl halide, $PdCl_2(PPh_3)_2$, K_2CO_3, DMF/H_2O, 100 °C (yields varied); (c) LiOH, $THF/CH_3OH/H_2O$; (d) TFA, CH_2Cl_2 (whenever the amino group of 'Ar' is protected by Boc).

as 3-pyridine (**14**), 2-pyrazine (**15**) or 4-*N*-methylpyrazole (**16**), attempting to capture possible interactions to the amino acid residues in the hinge region, did not improve the activity. However, a significant increase of potency was achieved when a basic moiety was appended to these heterocylces (**17–25**). An appropriate distance between the terminal amino group and the benzofuran core appears critical to achieve high potency, likely due to optimal interactions to *D128* and *E171* at the ribose binding region. This is evidenced by comparing the potency of compound **17** to **18,** as well as compound **25** to **21** and **22**. An X-ray crystal structure of **21** bound to the Pim-1 (Fig. 4a)[11] indicates an salt-bridge interaction with *D128* and water molecule mediated hydrogen bond interactions with *E171* by the terminal amino group. The pyrazine moiety of **21** is shown to be sitting in the position partially occupied by the bromo substituent of compound **10**, though it leans more towards the hinge site. No direct interaction of the pyrazine with amino acid residues in the hinge region could be identified in the crystal structures, an observation consistent with the aforementioned modest activities of compounds **14–16** (Table 1).

Analogs of compounds **11** were also prepared and their Pim-1 and Pim-2 inhibitory activities are summarized in Table 2. These analogs were designed to carry a basic moiety at the 7-position linker substituent in an attempt to capture interactions with *D128* and *E171*. Indeed, this structural modification resulted in significant increase of the potency in comparison to parent compound **11**. The nature of the linker does not seem to be very important, as demonstrated by comparing the activities of compound **26** to **29** and **33**, or compound **30** to **32** and **34** (Table 2). On the other hand, the basicity of the nitrogen center of the terminal amine is a significant factor impacting the potency, as evidenced by comparing the IC_{50} values of compounds **26** and **30** (terminal piperidine, $pK_a \sim 11$) to compounds **27** and **31** (terminal pyridine, $pK_a \sim 5$). Replacing the amino group with a hydroxyl (e.g., **38** to **40**, **39** to **41**) diminishes the activity which again highlights the importance of the salt-bridge interactions to *D128* and *E171* mediated by the terminal amino group (see Fig. 4).

In addition of the salt-bridge interactions with *D128* and *E171*, the X-ray structures of the bound complex of **38** (Fig. 4)[11] also reveals a hydrogen bond interactions with *N172* via a water bridge, though it is difficult to assess the importance of this interaction for the binding affinity. The position of the 5-bromo group of **38** almost coincides with the 5-bromo group of **11**. The concise and rigid *cis*-diamino-cyclohexanyl ring looked possessing an ideal shape to position the terminal amino residue in the right distance and orientation, allowing for strong interactions with *D128* and *E171*. The spatial arrangement could likely be the cause which makes this relatively small size molecule (**38**), with a molecular weight of 353, capable of strong binding and inhibition of both Pim-1 and Pim-2 as demonstrated by IC_{50}'s of 0.001 μM and 0.004 μM, respectively (Table 2). The LE of compound **38** is 0.59 (Table 2), which is significantly increased from the LE of the original hit molecule **11** (0.48, Fig. 2).

Compounds **12** and **13** of Table 1 were prepared according to literature procedures,[12] while the remaining compounds (**14–25**) in

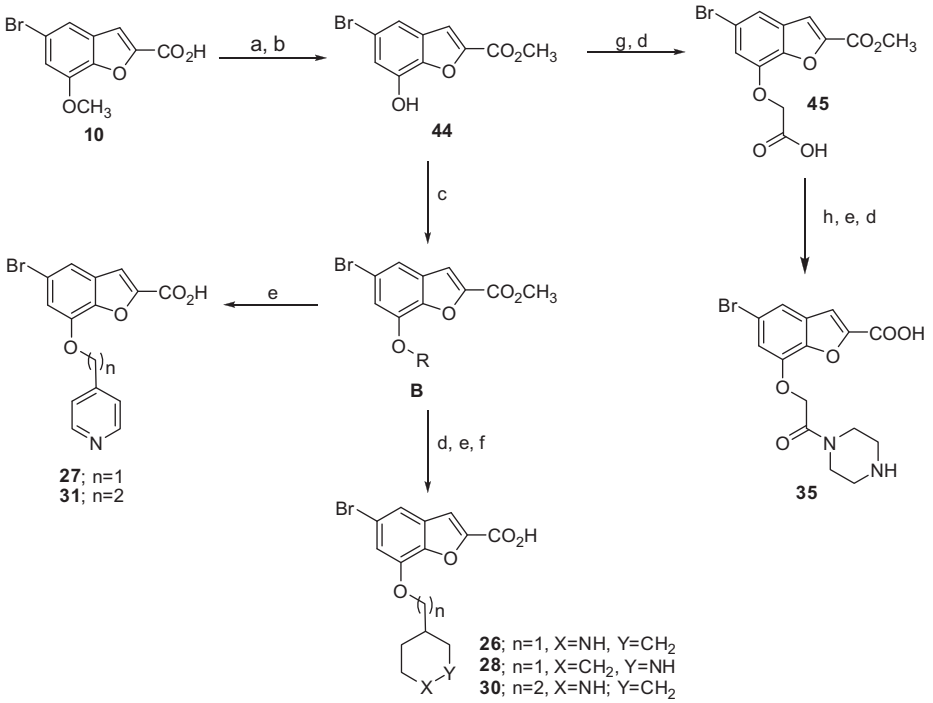

Scheme 2. Reagents and conditions: (a) BBr_3, CH_2Cl_2; (b) CH_3OH, cat. H_2SO_4, reflux (quant., two steps); (c) ROH, DEAD, PPh_3, EtOAc; (d) TFA, CH_2Cl_2; (e) LiOH, $THF/CH_3OH/H_2O$ (>90%); (f) HCl, H_2O; (g) *t*-butyl bromoacetate, K_2CO_3, DMF (97%); (h) *N*-Boc-piperazine, EDC, CH_2Cl_2 (79%).

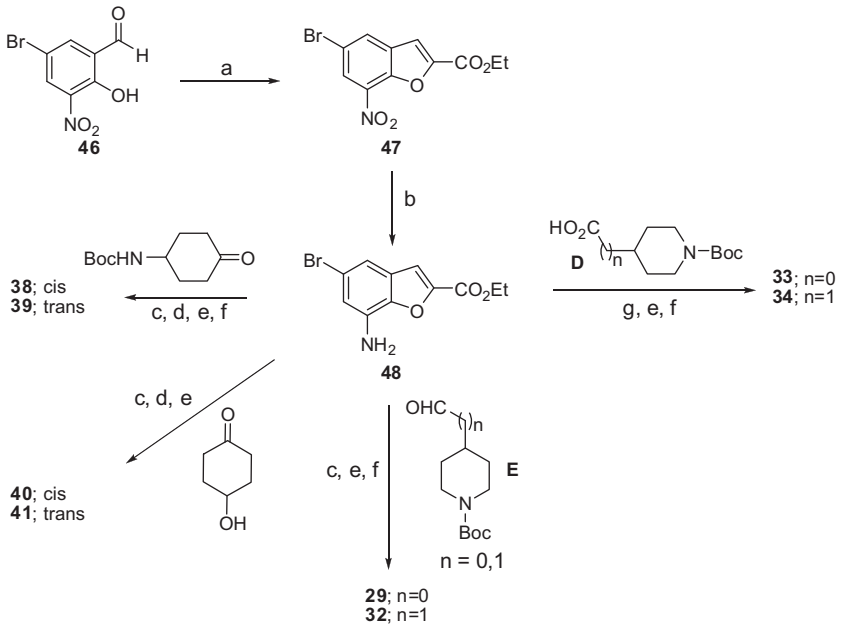

Scheme 3. Reagents and conditions: (a) diethyl bromomalonate, K_2CO_3, 2-butanone, reflux; (b) Fe, NH_4CI, $EtOH/H_2O$; (c) ketone/aldehyde, cat. AcOH, $NaBH(OAc)_3$, DCE; (d) *cis*/*trans* chromatographic resolution; (e) LiOH, $THF/CH_3OH/H_2O$; (f) TFA, CH_2CI_2; (g) carboxylic acid, HATU, DIEA, DMF (>70%).

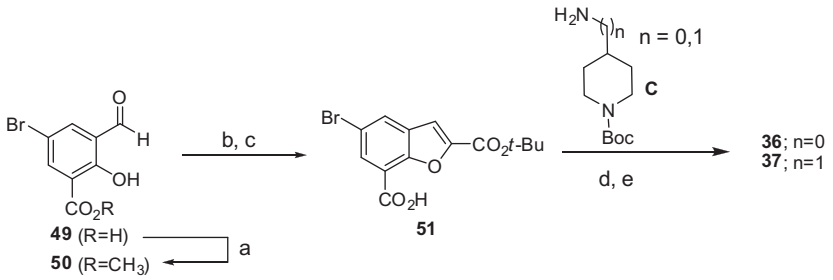

Scheme 4. Reagents and conditions: (a) CH_3OH, cat. H_2SO_4, reflux (47%); (b) di-*t*-butyl bromomalonate, K_2CO_3, 2-butanone, reflux (50%); (c) LiOH, $THF/CH_3OH/H_2O$ (16%); (d) amine, HATU, DIEA, DMF (80/25%); (e) TFA, CH_2CI_2 (100/42%.).

Table 1 were prepared as shown in Scheme 1. For example, ethyl 5-bromo-benzofuron-2-carboxylate (**42**) was converted to a boronic ester (**43**), which then was coupled with a variety of aryl halides to afford intermediate **A**. Upon hydrolysis with aqueous lithium hydroxide and, if necessary, deprotection of the Boc-amino group with acid, the desired compounds **14–25** were obtained. The compounds listed in Table 2 were prepared using the methods outlined in Schemes 2–4. For instance, in Scheme 2 compound **10** was converted to **44** by demethylation with BBr_3, followed by acid catalyzed esterification with methanol. Mitsunobu reaction of **44** with selected alcohols produced intermediate **B**, from which the desired acids (**26–28**, **30**, **31**) were prepared by conventional chemical transformations. The intermediate **44** was also used to prepare compound **35**. Thus, *O*-alkylation with *t*-butylbromoacetate followed by *t*-butyl cleavage afforded intermediate **45**, which was then subjected to EDC mediated amide formation, basic hydrolysis and, finally, Boc-deprotection to produce the target compound (**35**). Scheme 3 illustrates the synthesis of compounds **29**, **32–34**, **38–41** from a common intermediate **48**. The commercially available 5-bromo-2-hydroxy-3-nitrobenzaldehyde (**46**) was reacted with diethyl bromomalonate to form **47**, which was reduced to **48** by iron powder and ammonium chloride in aqueous ethanol. Standard reductive amination or amide coupling was used to attach the tailpiece followed by ester hydrolysis and/or amine deprotection completed the syntheses. The compounds **36** and **37** were prepared from the known intermediate 5-bromo-3-formyl-2-hydroxybenzoic acid (**49**)[13] using the following sequence as illustrated in Scheme 4: (a) conversion to methyl ester **50**; (b) reaction with *t*-butyl bromomalonate followed by selective hydrolysis to form **51**; (c) HATU mediated amide formation by coupling with *N*-Boc protected piperidinyl amines **C** and (d) simultaneous deprotection of the *N*-Boc and the *t*-butyl ester functionalities with TFA.

The active compounds have also been tested in a panel of *in vitro* ADME assays. Results for the three most potent Pim-1 inhibitors are summarized in Table 4. All three compounds were

Table 3
Ambit kinase selectivity data of compound **29**[a]

Ambit gene symbol	% Control
PIM1	**9.6**
PIM3	**13**
MYO3B	14
CSNK2A1	21
PIM2	**26**
CSNK2A2	28

[a] Compound **29** was tested in an Ambit 442 kinase panel at concentration of 100 nM.

Table 4
In vitro ADME data for selected Pim-1 inhibitors

Compds	MW	Sol., pH 7.4[a]	Microsomes rat CL_{int}[b]	Microsomes human CL_{int}[c]	1A2 IC_{50}[d]	2C9 IC_{50}[d]	2C19 IC_{50}[d]	2D6 IC_{50}[d]	3A4 IC_{50}[d]
29	353	>58	14.1	9.9	>10	>10	>10	>10	>10
38	353	20.1	10.0	10.2	>10	>10	>10	>10	>10
39	353	>58	8.1	11.2	>10	>10	>10	>10	>10

[a] Solubility measurement determined from DMSO stock at pH 7.4 in phosphate buffered saline, recorded as μg/mL.
[b] Metabolic stability in rat liver microsomes. Intrinsic clearance reported as μL/min/mg protein.
[c] Metabolic stability in human liver microsomes. Intrinsic clearance reported as μL/min/mg protein.
[d] Cytochrome P450 inhibition using human liver microsome and selected chemical probe substrates, reported as μM.

inactive against a set of five CYP isozymes, demonstrated adequate aqueous solubility and were moderately stable in rat and human liver microsome metabolic stability assays.

To assess the selectivity of the inhibitors, compound **29** was tested in an Ambit 442 kinase panel at a concentration of 100 nM, about five-fold higher than its IC_{50} value in the Pim-1 inhibition assay. Under these conditions, compound **29** inhibits, in addition to Pim-1, Pim-2 and Pim-3, only three non-Pim kinases (MYO3B, CSNK2A1 and CSNK2A2) for >50% of the binding (Table 3), indicating the good selective nature of this structural class against the Pim kinase family.

In summary, using fragment based screening against Pim-1 and X-ray structure guided medicinal chemistry optimization, we have identified novel benzofuran-2-carboxylic acid compounds which potently inhibit Pim-1 and Pim-2. These inhibitors have good selectivity as indicated by profiling compound **29** in an Ambit 442 kinase panel. The X-ray structures of these compounds bound to Pim-1 revealed important hydrogen bond interactions involving the 2-carboxylate group and the terminal amino group. The discovery of potent and selective Pim kinase inhibitors provides useful tools for the further evaluation of the role of this kinase family in the context of disease states and possible interventions in the treatment of cancer or other diseases.

References and notes

1. (a) Amaravadi, R.; Thompson, C. B. *J. Clin. Invest.* **2005**, *115*, 2618; (b) Magnuson, N. S.; Wang, Z.; Ding, G.; Reeves, R. *Future Oncol.* **2010**, *6*, 1461; (c) Nawijn, M. C.; Alendar, A.; Berns, A. *Nat. Rev. Cancer* **2011**, *11*, 23.
2. Cuypers, H. T.; Selten, G.; Quint, W.; Zijlstra, M.; Robanus-Manndag, E.; Boelens, W.; van Wezenbeek, P.; Berns, A. *Cell* **1984**, *37*, 141.
3. (a) Verbeek, S.; van Lohuizen, M.; van der Valk, M.; Domen, J.; Kraal, G.; Berns, A. *Mol. Cell. Biol.* **1991**, *11*, 1176; (b) Zhang, Y.; Wang, Z.; Li, X.; Magnuson, N. S. *Oncogene* **2008**, *27*, 4809; (c) Li, S.; Xi, Y.; Zhang, H.; Wang, Y.; Wang, X.; Liu, H.; Chen, K. *Oncol. Rep.* **2010**, *24*, 997; (d) Cen, B.; Mahajan, S.; Zemskova, M.; Beharry, Z.; Lin, Y. W.; Cramer, S. D.; Lilly, M. B.; Kraft, A. S. *J. Biol. Chem.* **2010**, *285*, 29128.
4. Amson, R.; Sigaux, F.; Przedborski, S.; Flandrin, G.; Givol, D.; Telerman, A. *Proc. Natl. Acad. Sci. U.S.A.* **1989**, *86*, 8857.
5. Cohen, A. M.; Grinblat, B.; Bessler, H.; Kristt, D.; Kremer, A.; Schwartz, A.; Halperin, M.; Shalom, S.; Merkel, D.; Don, J. *Leuk. Lymphoma* **2004**, *45*, 951.
6. (a) Kim, K. T.; Baird, K.; Ahn, J. Y.; Meltzer, P.; Lilly, M.; Levis, M.; Small, D. *Blood* **2005**, *105*, 1759; (b) Kim, K. T.; Levis, M.; Small, D. *Br. J. Haematol.* **2006**, *124*, 500.
7. Qian, K. C.; Wang, L.; Hickey, E. R.; Studts, J.; Barringer, K.; Peng, C.; Kronkaitis, A.; Li, J.; White, A.; Mische, S.; Farmer, B. *J. Biol. Chem.* **2005**, *280*, 6130.
8. (a) Tong, Y.; Stewart, K. D.; Thomas, S.; Przytulinska, M.; Johnson, E. F.; Klinghofer, V.; Leverson, J.; McCall, O.; Soni, N. B.; Luo, Y.; Lin, N. H.; Sowin, T. J.; Giranda, V. L.; Penning, T. D. *Bioorg. Med. Chem. Lett.* **2008**, *18*, 5206; (b) Tao, Z. F.; Hasvold, L. A.; Leverson, J. D.; Han, E. K.; Guan, R.; Johnson, E. F.; Stoll, V. S.; Stewart, K. D.; Stamper, G.; Soni, N.; Bouska, J. J.; Luo, Y.; Sowin, T. J.; Lin, N. H.; Giranda, V. S.; Rosenberg, S. H.; Penning, T. D. *J. Med. Chem.* **2009**, *52*, 6621; (c) Qian, K.; Wang, L.; Cywin, C. L.; Hickey, E.; Homon, C.; Jakes, S.; Kashem, M. A.; Lee, G.; Leonard, S.; Li, J.; Magboo, R.; Mao, W.; Pack, E.; Peng, C.; Welzel, M.; Wolak, J.; Morwick, T. *J. Med. Chem.* **2009**, *52*, 1814; (d) Pierce, A. C.; Jacobs, M.; Stuver-Moody, C. *J. Med. Chem.* **2008**, *52*, 1972; (e) Chen, L. S.; Redkar, S.; Bearss, D.; Wierda, W. G.; Gandhi, V. *Blood* **2009**, *114*, 4150; (f) Cheney, I. W.; Yan, S.; Appleby, T.; Walker, H.; Vo, T.; Yao, N.; Hamatake, R.; Hong, Z.; Wu, J. Z. *Bioorg. Med. Chem. Lett.* **2007**, *17*, 1679; (g) Grey, R.; Pierce, A. C.; Bemis, G. W.; Jacobs, M. D.; Moody, C. S.; Jajoo, R.; Mohal, N.; Green, J. *Bioorg. Med. Chem. Lett.* **2007**, *19*, 3019; (h) Pogacic, V.; Bullock, A. N.; Fedorov, O.; Filippakopoulos, P.; Gasser, C.; Biondi, A.; Meyer-Monard, S.; Knapp, S.; Schwaller, J. *Cancer Res.* **2007**, *67*, 6916.
9. Pim-1 protein was chemically minimally biotinylated with EZ-link Sulfo-NHS-LC-LC-biotin (Thermo Scientific) and removed of free biotin reagent by buffer exchanging 10 times with Amicon 3K Ultracel Membrane Ultra Centrifugal Filters (Millipore). All biosensor work was performed on a Biacore T100 instrument (GE Healthcare). NeutrAvidin (NA, Thermo Scientific) was amine coupled to the surface of a CM5 sensor chip to 8000–12,000 RU by standard methods. Biotinylated Pim-1 was captured onto the CM5-NA surface to 4000–6000 RU. Compounds were individually screened for binding at a final concentration of 75 μM at 4 °C. Steady-state affinities were determined for select compounds using similar assay conditions. Raw sensorgrams were double-referenced and solvent corrected with Biacore T100 Evaluation Software.
10. Human Pim-1(0.6 nM), Pim-2 (1.2 nM) or Pim-3 (0.6 nM) enzyme was pre-incubated with compound in a 100 mM Hepes pH 7.5 buffer containing 0.01% Triton X-100, 10 mM $MgCl_2$, 0.1% BSA, 1 mM DTT, 10 μM sodium orthovanadate, 10 μM beta-glycerophosphate and 1.25% DMSO for 15 min at room temperature. The reaction was initiated by addition of 1 μM peptide substrate (5-FAM-RSRHSSYPAGT-$CONH_2$, Caliper Life Sciences, MA) and 150 μM ATP for Pim-1, 3 μM ATP for Pim-2 or 25 μM ATP for Pim-3 assay. The reaction was incubated at room temperature for 45 min for Pim-1, 90 min for Pim-2 and Pim-3 and terminated with a 100 mM Hepes pH 7.5 buffer containing 100 mM EDTA, 0.02% Brij, 0.1% CR-3 and 0.36% DMSO. The reaction product was detected by one cycle run on a LabChip 3000 (Caliper Life Sciences) using an off-chip mobility shift protocol.
11. Purified Pim-1 protein (aa 29–313) with a C-terminal His tag was concentrated to 10–13 mg/ml in 20 mM HEPES, pH 8, 120 mM NaCl, 5 mM DTT. Pim-1 was crystallized in 0.1 M imidazole, pH 6.4, 1–1.4 M sodium acetate anhydrous by sitting drop vapor diffusion at 4 °C and reached maximum size after about 5 days. Pim-1 crystals were soaked with 1–10 mM compound in the well solution overnight at 4 °C and flash frozen with 30% glycerol in the presence of the compound. Diffraction data were collected at ALS503 (Advanced Light Source at Lawrence Berkeley National Laboratory, Berkeley, CA) and processed using HKL2000 and Scala. Crystals belong to space group $P6_5$, with $a = 98$ Å, $b = 98$ Å, $c = 80$ Å, $\alpha = 90.00$, $\beta = 90.00$, $\gamma = 120.00$. The structures were solved by molecular replacement using Molrep with PDB 1YWV as the search model. Iterative manual model building was carried out with Coot, coupled with refinement using Refmac5. For the crystal structures in complex with compound **21** and **38**, the Fo–Fc difference density indicates a peptide was bound. A tentative four residue peptide was build into the density and refined together with the Pim-1 structure. The X-ray coordinates of the structures of the bound complexes have been deposited in the RCSB protein data bank. They are 3R00 (structure a in Fig. 3), 3R01 (structure b in Fig. 3), 3R02 (structure b in Fig. 4) and 3R04 (structure a in Fig. 4).
12. Bernd, P.; Sonja, B.; Nielsen, R.; Kiuff, D.; Rimvall, K. *Bioorg. Med. Chem. Lett.* **2006**, *16*, 3162.
13. Ruell, J. A.; De Clerq, E.; Pannecouque, C.; Witvrouw, M.; Stup, T. L.; Turpin, J. A.; Buchheit, R. W.; Cushman, M. *J. Org. Chem.* **1999**, *64*, 5858.
14. Hopkins, A. L.; Groom, C. R.; Alex, A. *Drug Discovery Today* **2004**, *9*, 430.